REGULAR ARTICLE

blood advances

Clinicogenomic associations in childhood Langerhans cell histiocytosis: an international cohort study

Paul G. Kemps,[1,2] Timo C. E. Zondag,[3] Helga B. Arnardóttir,[4] Nienke Solleveld-Westerink,[1] Jelske Borst,[5] Eline C. Steenwijk,[5] Demi van Egmond,[1] Joost F. Swennenhuis,[6] Ellen Stelloo,[6] Irene Trambusti,[7] Robert M. Verdijk,[1,8] Carel J. M. van Noesel,[9] Arjen H. G. Cleven,[1,10] Marijn A. Scheijde-Vermeulen,[2] Marco J. Koudijs,[2] Lenka Krsková,[11] Cynthia Hawkins,[12] R. Maarten Egeler,[5] Jesper Brok,[13] Tatiana von Bahr Greenwood,[14,15] Karel Svojgr,[16] Auke Beishuizen,[2,17] Jan A. M. van Laar,[3,18] Ulrike Pötschger,[4] Caroline Hutter,[4] Elena Sieni,[7] Milen Minkov,[4] Oussama Abla,[19] Tom van Wezel,[1] Cor van den Bos,[2,20] and Astrid G. S. van Halteren[1,2]

[1]Department of Pathology, Leiden University Medical Center, Leiden, The Netherlands; [2]Princess Máxima Center for Pediatric Oncology, Utrecht, The Netherlands; [3]Department of Internal Medicine/Clinical Immunology, Erasmus Medical Center (Erasmus MC), Rotterdam, The Netherlands; [4]Children's Cancer Research Institute, St Anna Kinderkrebsforschung, Medical University of Vienna, Vienna, Austria; [5]Department of Pediatrics, Leiden University Medical Center, Leiden, The Netherlands; [6]Cergentis BV, Utrecht, The Netherlands; [7]Pediatric Hematology/Oncology Department, Meyer Children's University Hospital, Florence, Italy; [8]Department of Pathology, Erasmus MC University Medical Center Rotterdam, Rotterdam, The Netherlands; [9]Department of Pathology, Amsterdam University Medical Centers, Amsterdam, The Netherlands; [10]Department of Pathology, University Medical Center Groningen, Groningen, The Netherlands; [11]Department of Pathology and Molecular Medicine, Second Faculty of Medicine, Charles University and University Hospital Motol, Prague, Czech Republic; [12]Department of Pathology, The Hospital for Sick Children, University of Toronto, Toronto, ON, Canada; [13]Department of Pediatrics and Adolescent Medicine, Rigshospitalet, Copenhagen University Hospital, Copenhagen, Denmark; [14]Childhood Cancer Research Unit, Department of Women's and Children's Health, Karolinska Institutet, Stockholm, Sweden; [15]Department of Pediatric Oncology, Astrid Lindgren Children's Hospital, Karolinska University Hospital, Stockholm, Sweden; [16]Department of Pediatric Hematology and Oncology, Second Faculty of Medicine, Charles University and University Hospital Motol, Prague, Czech Republic; [17]Department of Pediatric Oncology, Sophia Children's Hospital, Erasmus MC, Rotterdam, The Netherlands; [18]Department of Immunology, Erasmus MC, Rotterdam, The Netherlands; [19]Department of Hematology/Oncology, The Hospital for Sick Children, University of Toronto, Toronto, ON, Canada; and [20]Department of Pediatric Oncology, Emma Children's Hospital, Amsterdam University Medical Centers, Amsterdam, The Netherlands

Key Points

- Oncogenic mutation subtype appears an important driver of heterogeneity in clinical presentation of pediatric LCH.
- Lesional *BRAF*^{V600E} status is not a significant prognostic factor for event-free survival independent from disease extent.

Langerhans cell histiocytosis (LCH) is a rare neoplastic disorder caused by somatic genetic alterations in hematopoietic precursor cells differentiating into CD1a^{+}/CD207^{+} histiocytes. LCH clinical manifestation is highly heterogeneous. *BRAF* and *MAP2K1* mutations account for ~80% of genetic driver alterations in neoplastic LCH cells. However, their clinical associations remain incompletely understood. Here, we present an international clinicogenomic study of childhood LCH, investigating 377 patients genotyped for at least *BRAF*^{V600E}. MAPK pathway gene alterations were detected in 300 (79.6%) patients, including 191 (50.7%) with *BRAF*^{V600E}, 54 with *MAP2K1* mutations, 39 with *BRAF* exon 12 mutations, 13 with rare *BRAF* alterations, and 3 with *ARAF* or *KRAS* mutations. Our results confirm that *BRAF*^{V600E} associates with lower age at diagnosis and higher prevalence of multisystem LCH, high-risk disease, and skin involvement. Furthermore, *BRAF*^{V600E} appeared to correlate with a higher prevalence of central nervous system (CNS)–risk bone lesions. In contrast, *MAP2K1* mutations associated with a higher prevalence of single-system (SS)-bone LCH, and *BRAF* exon 12 deletions seemed to correlate with more lung involvement. Although *BRAF*^{V600E} correlated with reduced event-free survival in the overall cohort, neither *BRAF* nor *MAP2K1* mutations associated with event-free survival when patients were stratified by disease extent. Thus, the correlation of *BRAF*^{V600E} with inferior clinical outcome is (primarily) driven by its association with disease extents known for high rates of progression or relapse, including multisystem LCH. These findings advance our understanding of factors underlying the remarkable clinical heterogeneity of LCH but also question the independent prognostic value of lesional *BRAF*^{V600E} status.

Submitted 26 April 2022; accepted 28 August 2022; prepublished online on *Blood Advances* First Edition 9 September 2022. https://doi.org/10.1182/bloodadvances.2022007947.

Data are available on request from the corresponding authors, Astrid G.S. van Halteren (a.vanhalteren@erasmusmc.nl) and Cor van den Bos (c.vandenbos-5@prinsesmaximacentrum.nl).

The full-text version of this article contains a data supplement.

Introduction

Langerhans cell histiocytosis (LCH) is a rare hematologic neoplasm characterized by the accumulation of myeloid-differentiated cells with characteristic CD1a and CD207 expression in various tissues and organs.[1-3] This disease primarily affects children, with an incidence similar to pediatric Hodgkin lymphoma.[4] The clinical manifestation of LCH is highly heterogeneous, ranging from self-healing skin lesions or a solitary bone lesion to a life-threatening disease involving multiple organ systems (supplemental Figure 1).[5] Disease extent is an established prognostic factor in pediatric LCH.[6-8] The most severe clinical form of the disease tends to affect young children (aged <2 years) and typically involves risk organs (ROs), including the hematopoietic system, liver, and spleen.[9,10] LCH with RO involvement is often refractory to chemotherapy and associated with an increased risk of death; therefore, it is called "high-risk LCH."[11-13] Although overall mortality of patients with LCH is low, a significant proportion of them experiences disease relapses[14] and/or develops permanent consequences, such as diabetes insipidus (DI) or neurodegenerative (ND)-LCH. Currently, the biological mechanisms underlying the heterogeneous clinical presentation and outcome of LCH remain incompletely understood.

In 2010, Rollins and colleagues discovered recurrent somatic *BRAF*^{V600E} mutations in LCH.[15] Subsequently, other groups confirmed the presence of *BRAF*^{V600E} mutations in ~50% to 60% of patients with LCH,[10,16-20] and identified alternative MAPK pathway–activating genetic alterations in patients without *BRAF*^{V600E} (supplemental Figure 2).[17,21-28] Most notably, somatic mutations in *MAP2K1* exon 2 or 3 and small insertions and/or deletions (indels) in *BRAF* exon 12 were recurrently detected.[17,22-25] Together, *BRAF* and *MAP2K1* mutations seem to account for ~80% of genetic driver alterations in pediatric LCH.[29] *BRAF*^{V600E}, *MAP2K1*, and *BRAF* exon 12 mutations are essentially mutually exclusive,[22] with only very rare cases having co-occurring mutations.[30,31]

In 2016, Héritier et al reported that *BRAF*^{V600E} associated with high-risk disease and increased rates of first-line therapy resistance and relapse in 315 patients with pediatric LCH,[10] including 173 children (54.6%) with *BRAF*^{V600E}. Since then, no study has been published with similar or more patients with LCH genotyped for *BRAF*^{V600E}. Hence, their observations still need to be duly confirmed. Moreover, large cohort studies with molecular data beyond *BRAF*^{V600E} are needed to determine the clinical impact of recurrent mutations in *MAP2K1* or *BRAF* exon 12, which remain largely unknown.[29] Accordingly, here we describe an international clinicogenomic study of childhood LCH, investigating 377 patients genotyped for at least *BRAF*^{V600E}, including 300 (79.6%) patients with a detected MAPK pathway gene alteration.

Materials and methods

Study design

We performed an international observational cohort study of clinical associations of somatic genetic alterations in pediatric LCH. Patients were included between 2014 and 2021 in a retrospective cohort study of patients with LCH in 4 academic children's hospitals in The Netherlands and Canada, or they were enrolled between 2013 and 2021 in the prospective LCH-IV clinical study (#NCT02205762/EudraCT 2011-001699-20) in The Netherlands, Italy, Austria, Czech Republic, Sweden, or Denmark. The study was performed in accordance with the Declaration of Helsinki, and ethical approval or a waiver of consent for retrospective research was obtained from the institutional review boards at participating institutions. Written informed consent was obtained from patients and/or their legal representatives when required. Inclusion of patients from the LCH-IV study was approved by the Data and Safety Monitoring Committee (DSMC). Inclusion stopped April 30 2021.

Patient selection and data collection

Patients were identified through registries of involved institutions. Eligibility criteria were (i) a definitive diagnosis of LCH, (ii) age at LCH diagnosis below 18 years, and (iiia) available LCH-lesional *BRAF*^{V600E} status by polymerase chain reaction (PCR) or sequencing through routine molecular diagnostics or (iiib) availability of formalin-fixed paraffin-embedded (FFPE) LCH tissue for molecular analysis in the specific context of this study. Diagnosis of LCH was confirmed by a combination of clinical findings and the presence of CD1a^{+} histiocytes in the lesional tissue sample(s). For patients with isolated skin disease, LCH diagnosis also required confirmation of CD207 coexpression by CD1a^{+} histiocytes, to rule out indeterminate cell histiocytosis, a diagnostic pitfall.[32] Patients enrolled in the prospective LCH-IV study were staged, treated, and followed up according to study protocol; other patients were managed according to standard-of-care. Importantly, first-line treatment and follow-up of patients were irrespective of mutational status; no patient received first-line therapy with BRAF and/or MEK inhibitors. Details of data collection are provided in the supplemental Methods.

Disease extent was categorized according to the classification of the LCH Study Group of the Histiocyte Society,[9] differentiating between single-system (SS) and multisystem (MS) disease. Within these categories, detailed subtypes were distinguished based on the type of organ(s) involved and/or the manifestation as unifocal or multifocal disease. The hematopoietic system, liver, and spleen were considered ROs,[9,33] and bone lesions affecting the orbital, temporal/mastoid, sphenoidal, zygomatic, ethmoidal bones, the maxilla, paranasal sinuses, or anterior or middle cranial fossa were considered central nervous system (CNS)–risk lesions.[9,34-36] LCH with RO involvement was termed "high-risk LCH." Event was defined as disease progression, LCH relapse, or death from any cause. Disease progression was defined as (1) insufficient response and/or progression of existing LCH manifestations requiring the start or a second- or further-line of chemotherapy, targeted therapy, and/or radiotherapy or (2) the development of new lesions in the presence of active disease. Disease relapse was defined as the development of new lesions after complete remission of prior LCH manifestations.

Molecular pathologic analysis

Molecular analysis was performed as part of routine diagnostics and/or in the specific context of this study. Importantly, none of the tissue samples were analyzed by BRAF VE1 immunohistochemistry alone. For (additional) molecular analysis performed in the context of this study, manual microdissection of LCH-lesional FFPE tissue sections was performed based on a CD1a-stained reference slide to obtain representative tissue parts enriched for neoplastic LCH cells,[37]

thereby increasing the success rate of mutation detection.[38] Automated DNA isolation from the microdissected tissue fragments and *BRAF*^{V600E} allele–specific real-time PCR and/or droplet digital PCR were performed as previously described.[39-41] When possible, cases without *BRAF*^{V600E} were further analyzed using Sanger sequencing and/or a custom-designed AmpliSeq next-generation sequencing (NGS) panel containing primers to detect mutations in *MAP2K1* (NM_002755.3) exon 2 to 3 and *BRAF* (NM_004333.6) exon 12 and 15, as well as in *ARAF*, *MAP3K1*, *N/KRAS*, and many other cancer-associated genes (supplemental Methods).[42] Finally, a small proportion of patients without *BRAF*^{V600E} was analyzed for alternative *BRAF* alterations by FFPE-targeted locus capture (FFPE-TLC) NGS,[43,44] a DNA-based technique able to identify both small variants (eg, single nucleotide variants or small indels) and structural variants (eg, gene rearrangements). Details are available in the supplemental Methods.

Statistical analysis

Comparisons of (sub)groups were performed using the 2-sided Mann-Whitney *U* or Kruskal-Wallis test for continuous data and 2-sided Fisher or Fisher-Freeman-Halton exact test for categorical data. In general, threshold for significance was $P < .05$; however, in univariable analysis of LCH presentation according to mutational status $P < .00125$ was considered statistically significant (Bonferroni correction for multiple testing).[10] In addition to significant results, findings insignificant after Bonferroni correction but with $P < .05$ were highlighted. These represent potential associations but with insufficient statistical evidence in this study and will require further careful evaluation to determine their potential clinical relevance. Variables significant after correction were included in a multivariable binary logistic regression analysis to identify the factor(s) most associated with *BRAF*^{V600E} after adjustment for the other variables. For hierarchical categorical variables (eg, bone-to-bone subtypes), the primary variable was considered for inclusion (eg, bone). Because RO involvement was restricted to MS LCH, liver and hematopoietic system involvement, both significant in univariable analysis, were not included as independent variables but instead MS-RO^{+} LCH was added as disease extent category to the regression model. Univariable survival analyses were performed using the Kaplan-Meier method, and survival curves were compared using the log-rank test. Event-free survival (EFS) was defined as the time from diagnosis until the first event or, for cases without an event, the date of last follow-up. To investigate how much of the effect of *BRAF*^{V600E} on EFS was mediated by disease extent, univariable survival analyses were stratified by disease extent and multivariable survival analysis was performed using Cox regression. Median follow-up was estimated using the reverse Kaplan-Meier method.[45] Incidences of DI, ND-LCH, specific sites of disease, chemotherapy, and second-line systemic therapy were indicated by proportions[10] because of incomplete time-to-event data for cumulative incidence calculations. Statistical analyses were performed using GraphPad Prism version 9.0.1 or IBM SPSS Statistics version 25.

Results

A total of 377 patients with childhood LCH and available *BRAF*^{V600E} status were included. This cohort comprised 198 (52.5%) patients from the prospective LCH-IV study and 179 (47.5%) patients from a Dutch/Canadian retrospective study, with comparable clinical characteristics (supplemental Table 1). The combined cohort comprised 222 (58.9%) males and 155 (41.1%) females. Median age at diagnosis was 3.6 years (range, 0.0-17.9 years). Patients could be classified into 288 (76.4%) patients with SS LCH and 89 (23.6%) patients with MS LCH. Patients with SS LCH could be categorized into 184 patients with unifocal bone disease (SS-UFB), 64 patients with multifocal bone disease (SS-MFB), 32 patients with isolated skin disease (SS-skin), and 8 patients with isolated involvement of another organ system, including the lungs (n = 3), lymph nodes (n = 3), CNS (n = 1), or soft tissue (n = 1). Patients with MS LCH could be divided into 55 patients without RO involvement (MS-RO^{-}) and 34 patients with RO involvement (MS-RO^{+} or high-risk LCH).

MAPK pathway gene alterations were detected in 300 out of 377 (79.6%) patients, including 191 (50.7%) with *BRAF*^{V600E} (Table 1). In the subgroup without *BRAF*^{V600E}, *MAP2K1* mutations were identified in 54 patients and *BRAF* exon 12 indels were detected in 39 children (Table 2). *MAP2K1* mutations occurred in exon 2 in 36 out of 54 (66.7%) patients and in exon 3 in 18 out of 54 (33.3%) patients. *BRAF* exon 12 indels included small in-frame deletions at the beginning of exon 12 affecting the β3-αC loop in 27 out of 39 (69.2%) patients and in-frame insertions of 9 nucleotides at the end of exon 12 affecting the αC-β4 loop in 12 out of 39 (30.8%) patients.[25,46-48] In the remaining patients in the *BRAF*$^{V600E-}$ group, *BRAF* exon 15 mutations other than *BRAF*^{V600E} (n = 10), *BRAF* fusions (n = 3), *ARAF* mutations (n = 2), and a *KRAS* mutation (n = 1) were detected (supplemental Table 2).

BRAF^{V600E} status in relation to clinical presentation

BRAF^{V600E} correlated with demographic characteristics, disease extent, and specific sites of disease at diagnosis (Figure 1; Table 1; supplemental Table 3). Patients with *BRAF*^{V600E} were significantly younger than patients without *BRAF*^{V600E} (median age, 2.6 years vs 5.7 years; $P < .001$). In addition, patients with *BRAF*^{V600E} more often had MS LCH (33.5% vs 13.4%; $P < .001$; Figure 1A) and high-risk disease (14.1% vs 3.8%; $P < .001$). Regarding sites of disease, *BRAF*^{V600E} significantly associated with more involvement of the skin ($P < .001$), liver ($P < .001$), and hematopoietic system ($P = .001$), and with less involvement of the upper extremity bones ($P = .001$; Figure 1B). Within SS-skin LCH, *BRAF*^{V600E} was significantly associated with multifocal skin involvement ($P = .001$; Figure 1C).

Concerning potential associations, *BRAF*^{V600E} seemed associated with less SS-MFB disease ($P = .006$; Figure 1A). Furthermore, *BRAF*^{V600E} appeared to correlate with a higher prevalence of spleen involvement ($P = .017$), gastrointestinal involvement ($P = .015$; Table 1), and CNS-risk bone lesions ($P = .011$; Figure 1B). When analyzing sites of disease during entire follow-up, including at LCH progression and/or relapse, these potential associations remained apparent (supplemental Figure 3; supplemental Table 4).

In multivariable analysis with age, disease extent (categorized as SS/MS-RO^{-}/MS-RO^{+} LCH), and skin involvement as independent variables (supplemental Table 5A), *BRAF*^{V600E} was significantly associated with skin involvement (odds ratio [OR], 2.23; 95% confidence interval [CI], 1.16-4.29; $P = .017$). However, OR was highest for MS-RO^{+} disease extent (OR, 2.54; 95% CI, 0.99-6.54; $P = .05$). In a regression model with age, MS disease (irrespective of RO status), and skin involvement as independent variables,

Table 1. Clinical characteristics according to *BRAF*^{V600E} status

	BRAF^{V600E+}	*BRAF*$^{V600E-}$	Odds ratio (95% confidence interval)	*P* value
Patients, n	191	186		
Age at diagnosis, y, median (range)	2.6 (0.0-17.6)	5.7 (0.0-17.9)	N/A	<.001††
Age <3 y, n (%)	105 (55.0)	66 (35.5)	2.22 (1.47-3.36)	<.001††
Age ≥3 y, n (%)	86 (45.0)	120 (64.5)		
Sex, n (%)				
Male	113 (59.2)	109 (58.6)	1.02 (0.68-1.54)	.92
Female	78 (40.8)	77 (41.4)		
Disease extent at diagnosis, n (%)				
MS	64 (33.5)	25 (13.4)	3.25 (1.93-5.45)	<.001††
SS	127 (66.5)	161 (86.6)		
Detailed subtype, n (%)*				
MS-RO^{+}	27 (14.1)	7 (3.8)	4.21 (1.79-9.93)	<.001††
MS-RO^{-}	37 (19.4)	18 (9.7)	2.24 (1.23-4.10)	.009**
SS-bone	109 (57.1)	139 (74.7)	0.45 (0.29-0.70)	<.001††
• SS-UFB	87 (45.5)	97 (52.2)	0.77 (0.51-1.15)	.22
• SS-UFB, CNS-risk†	16 (8.4)	19 (10.2)	0.80 (0.40-1.62)	.60
• SS-MFB	22 (11.5)	42 (22.6)	0.45 (0.26-0.78)	.006**
SS-skin	18 (9.4)	14 (7.5)	1.28 (0.62-2.65)	.58
SS-other	0 (0.0)	8 (4.3)¶	N/A	.003**
Disease site(s) at diagnosis, n (%)				
Bone	157 (82.2)	159 (85.5)	0.78 (0.45-1.36)	.41
• MFB lesions	56 (29.3)	55 (29.6)	0.99 (0.63-1.54)	1
• CNS-risk bone lesion(s)†	64 (33.5)	40 (21.5)	1.84 (1.16-2.92)	.011**
• Spinal column lesion(s)	18 (9.4)	28 (15.1)	0.59 (0.31-1.10)	.12
Skin	69 (36.1)	24 (12.9)	3.82 (2.27-6.43)	<.001††
Liver‡	24 (12.6)	5 (2.7)	5.20 (1.94-13.95)	<.001††
Hematopoietic system‡	19 (9.9)	3 (1.6)	6.74 (1.96-23.18)	.001††
Spleen‡	15 (7.9)	4 (2.2)	3.88 (1.26-11.91)	.017**
Lymph node	17 (8.9)	17 (9.1)	0.97 (0.48-1.97)	1
Lung	10 (5.2)	14 (7.5)	0.68 (0.29-1.57)	.40
CNS§	8 (4.2)	4 (2.2)	1.99 (0.59-6.72)	.38
Gastrointestinal tract	7 (3.7)	0 (0.0)	N/A	.015**
Follow-up, y, median (range)	4.0 (0.0-38.8)	3.8 (0.0-36.0)	N/A	.61#
Permanent consequences developed during follow-up, n (%)				
DI	23 (12.0)	14 (7.5)	1.68 (0.84-3.38)	.17
ND-LCH‖	5 (2.6)	0 (0.0)	N/A	.06
Death, n	4	4	N/A	.97#

N/A, not available.

*Fisher exact tests comparing patients with vs without a disease extent subtype are shown. Fisher-Freeman-Halton exact test comparing proportions in all different subgroups (a contingency table larger than 2 × 2) is not shown but was significant ($P < .001$).

†Bone lesions affecting the orbital, temporal/mastoid, sphenoidal, zygomatic, or ethmoidal bones, the maxilla, paranasal sinuses, or anterior or middle cranial fossa.

‡These organs are considered ROs.

§Given that the posterior pituitary and pituitary stalk are direct extensions of the hypothalamus, pituitary tumors are classified as CNS involvement. All 12 patients with CNS involvement at diagnosis had tumorous lesions, for example, pituitary stalk lesions.

‖Only patients with both clinical and radiologic ND-LCH are reported.

¶These 8 patients comprised 3 patients with SS-lung LCH, 3 patients with SS-lymph node LCH, and single cases with SS-soft tissue or (tumorous) SS-CNS disease.

#Obtained with the log-rank test.

**$P < .05$.

††$P < .00125$ (Bonferroni correction for multiple testing; tests are shown in this table and supplemental Table 3).

Table 2. Clinical characteristics of patients with *MAP2K1* or *BRAF* exon 12 mutations

	MAP2K1 mutated			*BRAF* exon 12 mutated		
	***MAP2K1* exon 2**	***MAP2K1* exon 3**	**All patients**	**In-frame deletions**	**In-frame insertions**	**All patients**
Patients, n	36	18	54	27	12	39
Age at diagnosis, y, median (range)	2.7 (0.0-15.1)	8.3 (1.7-17.1)	4.8 (0.0-17.1)	3.4 (0.2-17.9)	6.2 (0.5-14.4)	5.9 (0.2-17.9)
Age <3 y, n (%)	19 (52.8)	1 (5.6)	20 (37.0)	12 (44.4)	3 (25.0)	15 (38.5)
Age ≥3 y, n (%)	17 (47.2)	17 (94.4)	34 (63.0)	15 (55.6)	9 (75.0)	24 (61.5)
Sex, n (%)						
Male	23 (63.9)	10 (55.6)	33 (61.1)	16 (59.3)	5 (41.7)	21 (53.8)
Female	13 (36.1)	8 (44.4)	21 (38.9)	11 (40.7)	7 (58.3)	18 (46.2)
Disease extent at diagnosis, n (%)						
MS	3 (8.3)	1 (5.6)	4 (7.4)	7 (25.9)	1 (8.3)	8 (20.5)
SS	33 (91.7)	17 (94.4)	50 (92.6)	20 (74.1)	11 (91.7)	31 (79.5)
Detailed subtype, n (%)						
MS-RO^{+}	1 (2.8)	0 (0.0)	1 (1.9)	3 (11.1)	0 (0.0)	3 (7.7)
MS-RO^{-}	2 (5.6)	1 (5.6)	3 (5.6)	4 (14.8)	1 (8.3)	5 (12.8)
SS-bone	30 (83.3)	16 (88.9)	46 (85.2)	15 (55.6)	11 (91.7)	26 (66.7)
• SS-UFB	22 (61.1)	13 (72.2)	35 (64.8)	11 (40.7)	8 (66.7)	19 (48.7)
• SS-UFB, CNS-risk	4 (11.1)	1 (5.6)	5 (9.3)	4 (14.8)	2 (16.7)	6 (15.4)
• SS-MFB	8 (22.2)	3 (16.7)	11 (20.4)	4 (14.8)	3 (25.0)	7 (17.9)
SS-skin	3 (8.3)	0 (0.0)	3 (5.6)	2 (7.4)	0 (0.0)	2 (5.1)
SS-other	0 (0.0)	1 (5.6)	1 (1.9)	3 (11.1)	0 (0.0)	3 (7.7)
Disease site(s) at diagnosis, n (%)						
Bone	33 (91.7)	17 (94.4)	50 (92.6)	20 (74.1)	12 (100)	32 (82.1)
• MFB lesions	11 (30.6)	3 (16.7)	14 (25.9)	7 (25.9)	3 (25.0)	10 (25.6)
• CNS-risk bone lesion(s)	8 (22.2)	1 (5.6)	9 (16.7)	8 (29.6)	3 (25.0)	11 (28.2)
• Spinal column lesion(s)	6 (16.7)	2 (11.1)	8 (14.8)	5 (18.5)	2 (16.7)	7 (17.9)
Skin	5 (13.9)	0 (0.0)	5 (9.3)	6 (22.2)	0 (0.0)	6 (15.4)
Liver	0 (0.0)	0 (0.0)	0 (0.0)	3 (11.1)	0 (0.0)	3 (7.7)
Hematopoietic system	1 (2.8)	0 (0.0)	1 (1.9)	1 (3.7)	0 (0.0)	1 (2.6)
Spleen	0 (0.0)	0 (0)	0 (0.0)	2 (7.4)	0 (0.0)	2 (5.1)
Lymph node	2 (5.6)	2 (11.1)	4 (7.4)	4 (14.8)	1 (8.3)	5 (12.8)
Lung	1 (2.8)	0 (0.0)	1 (1.9)	6 (22.2)	0 (0.0)	6 (15.4)
CNS	1 (2.8)	0 (0.0)	1 (1.9)	1 (3.7)	0 (0.0)	1 (2.6)
Follow-up, y, median (range)	2.7 (0.2-15.2)	4.3 (1.4-30.4)	3.7 (0.2-30.4)	6.3 (0.4-27.0)	3.5 (0.7-9.4)	5.3 (0.4-27.0)
Permanent consequences developed during follow-up, n (%)						
DI	1 (2.8)	1 (5.6)	2 (3.7)	5 (18.5)	0 (0.0)	5 (12.8)
Death, n	2	0	2	2	0	2

BRAF^{V600E} was significantly associated with both MS disease and skin involvement (supplemental Table 5B).

MAP2K1 and *BRAF* exon 12 mutations in relation to clinical presentation

MAP2K1 mutations also correlated with clinical features at diagnosis (Figure 2; supplemental Table 6). Compared with children with *BRAF*^{V600E}, patients with *MAP2K1* mutations had significantly more SS-bone LCH (85.2% vs 57.1%; $P < .001$; Figure 2D) and less MS LCH (7.4% vs 33.5%; $P < .001$; Figure 2E) and skin involvement (9.3% vs 36.1%; $P < .001$; Figure 2G). *MAP2K1* mutations also appeared to correlate with more SS-bone disease when compared with *BRAF* exon 12 mutations ($P = .045$; Figure 2D), particularly compared with *BRAF* exon 12 deletions affecting the β3-αC loop ($P = .006$; supplemental Figure 4B). Regarding subtypes of bone involvement, patients with *MAP2K1* mutations had the lowest prevalence of CNS-risk bone lesions, despite having the most bone involvement (Figure 2F). Children with *MAP2K1* mutations did have the highest prevalence of bone lesions in the upper extremities and/or shoulder girdle (supplemental Figure 5). Regarding demographic characteristics, *MAP2K1* mutations appeared to correlate with older age at diagnosis when compared with *BRAF*^{V600E} ($P = .011$; Figure 2B).

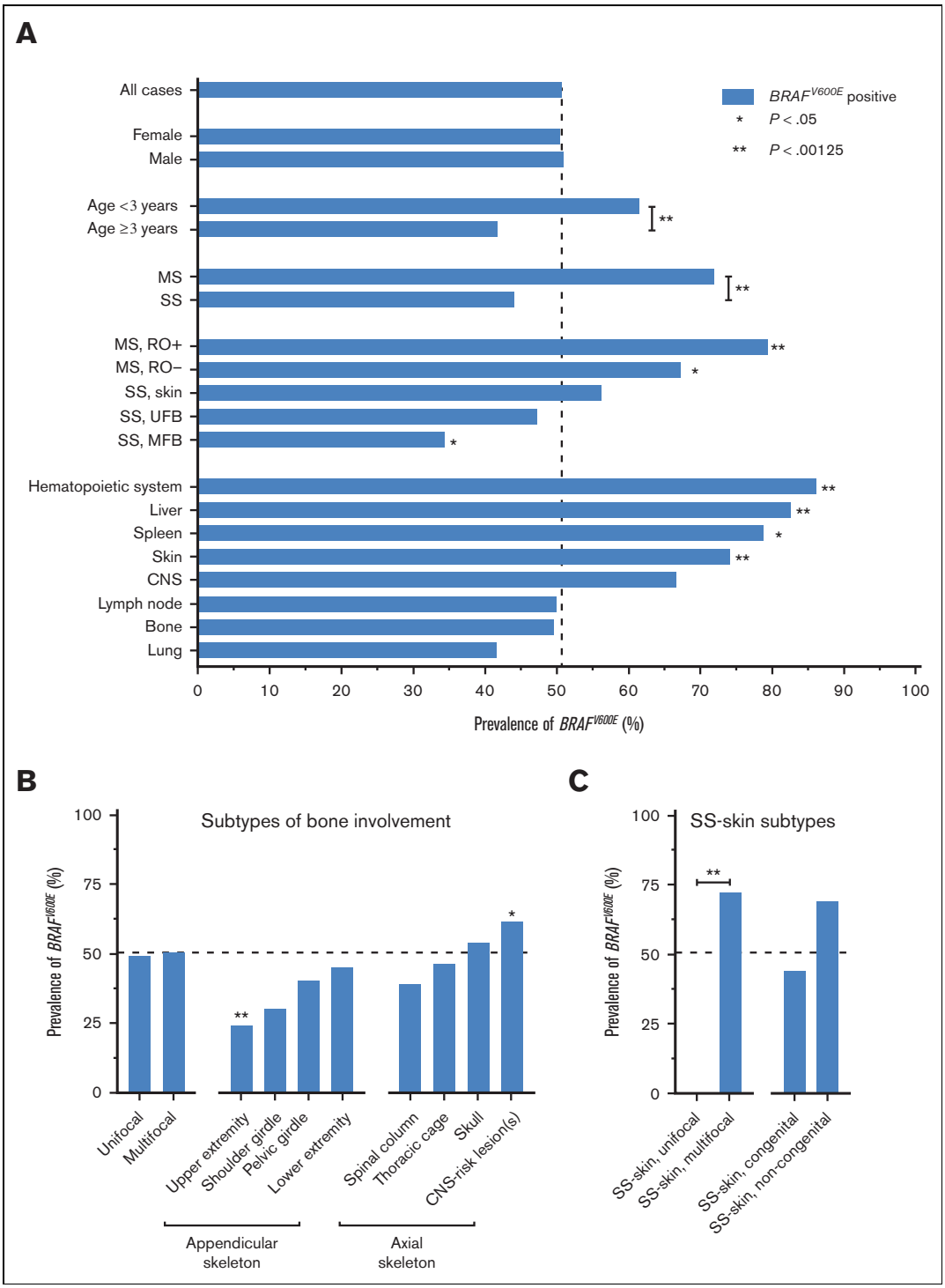

Figure 1. Clinical features at LCH diagnosis according to *BRAF*^{V600E} status. (A) Prevalence of *BRAF*^{V600E} in patients with specific clinical characteristics at LCH diagnosis. (B) Prevalence of *BRAF*^{V600E} in patients with specific types of bone involvement at diagnosis. This figure depicts all patients with osseous lesions, irrespective of single-systemic or multisystemic disease extent. Bones are grouped according to the classification used by the National Cancer Institute. Upper extremity: humerus, radius, ulna, carpals, metacarpals, and phalanges. Shoulder girdle: clavicle and scapula. Pelvic girdle: coxal, innominate, and hip bones (including ilium, ischium, acetabulum, and pubis). Lower extremity: femur, tibia, fibula, patella, tarsals, metatarsals, and phalanges. Spinal column: cervical, thoracic and lumbar vertebrae, sacrum, and coccyx. Thoracic cage: ribs and sternum. CNS-risk lesions are bone lesions affecting the orbital, temporal/mastoid, sphenoidal, zygomatic, or ethmoidal bones, the maxilla, paranasal sinuses, or anterior or middle cranial fossa, according to LCH Study Group definitions.[9,34-36] (C) Prevalence of *BRAF*^{V600E} in patients with specific presentations of SS-skin LCH at diagnosis. Numbers of patients are provided in Table 1 and supplemental Table 3. Dashed lines indicate the prevalence of *BRAF*^{V600E} in all cases (51%). Statistical tests with $P < .05$ are shown. *$P < .05$, **$P < .00125$. MS, multisystem; SS, single-system; RO, risk organ; UFB, unifocal bone; MFB, multifocal bone; CNS, central nervous system.

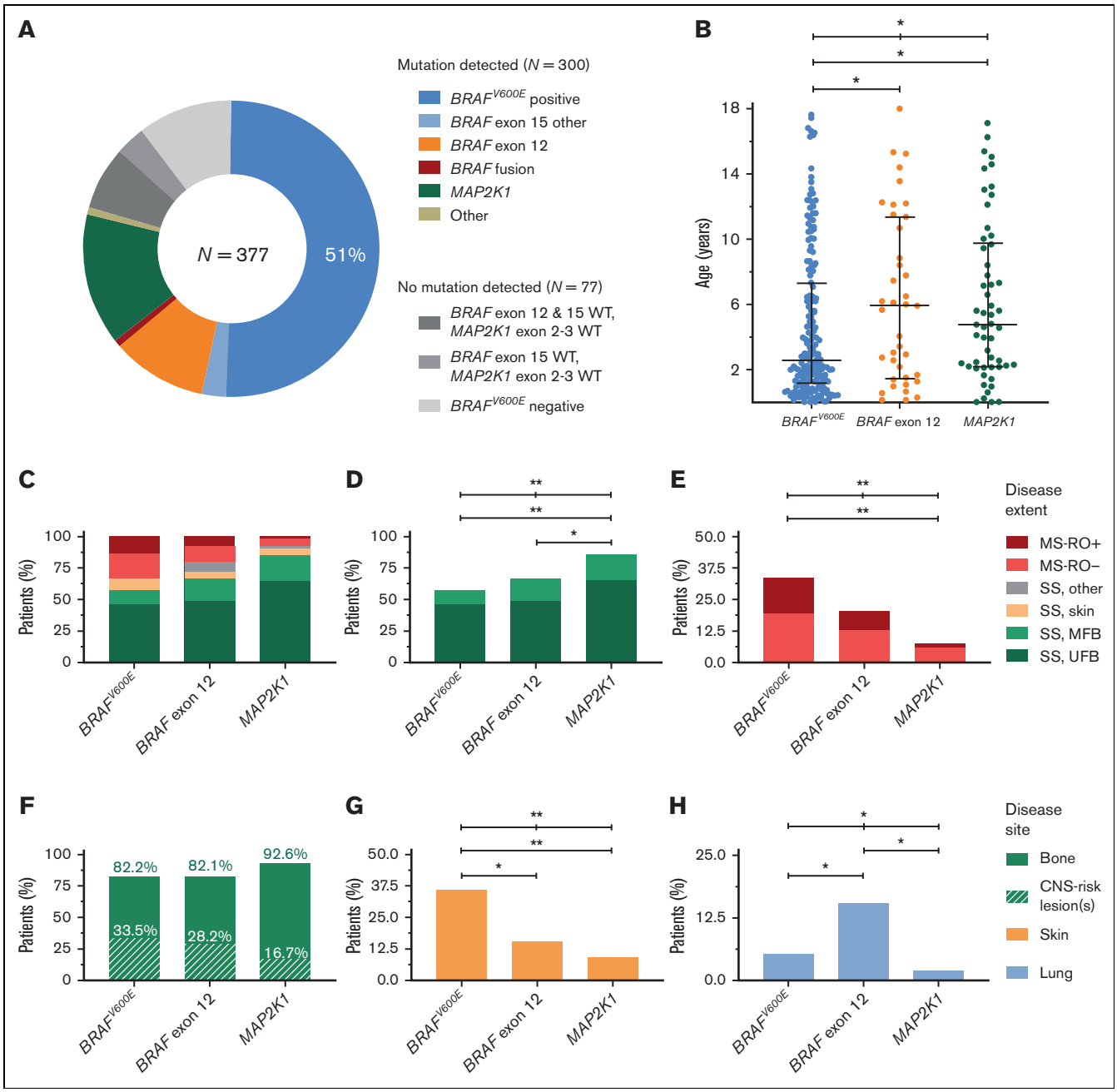

Figure 2. Clinical features at LCH diagnosis of children with *BRAF*^{V600E}, *BRAF* exon 12, or *MAP2K1* mutations. (A) Pie chart showing the mutational status of the 377 patients from our cohort. (B) Dot plot showing age at diagnosis of patients with *BRAF*^{V600E}, *BRAF* exon 12, or *MAP2K1* mutations. Error bars depict medians with interquartile ranges. (C-E) Bar charts depicting the percentage of patients with *BRAF*^{V600E}, *BRAF* exon 12, or *MAP2K1* mutations having specific disease extents at LCH diagnosis. Statistical comparisons were performed for SS-bone disease in panel D and MS disease in panel E. (F-H) Bar charts depicting the percentage of patients with *BRAF*^{V600E}, *BRAF* exon 12, or *MAP2K1* mutations having specific disease sites at LCH diagnosis. Statistical tests with $P < .05$ are depicted. Numbers of patients are provided in Tables 1 and 2. *$P < .05$, **$P < .00125$. WT, wild-type.

Similar to what was observed for *MAP2K1* mutations, *BRAF* exon 12 indels seemed associated with older age at diagnosis ($P = .049$; Figure 2B) and less skin involvement ($P = .014$; Figure 2G) when compared with *BRAF*^{V600E}. Furthermore, *BRAF* exon 12 mutations appeared to correlate with a higher prevalence of lung involvement when compared with *BRAF*^{V600E} ($P = .035$) or *MAP2K1* mutations ($P = .020$; Figure 2H). Pulmonary involvement was particularly frequent in patients with *BRAF* exon 12 deletions affecting the β3-αC loop (6/27 [22.2%]; supplemental Figure 4F). Notably, *BRAF* exon 12 deletions were also detected in 3 out of 7 patients (43%) with thymic involvement[49-51]; the other 4 patients had alternative *BRAF* alterations (supplemental Figure 6).

BRAF^{V600E} status in relation to clinical outcome

Follow-up was similar for patients with *BRAF*^{V600E} and patients without *BRAF*^{V600E} (median, 4.0 years vs 3.8 years; $P = .61$). In the overall cohort, children with *BRAF*^{V600E} had significantly reduced EFS (5-year EFS, 54.1%; standard error ± 4.4% vs 59.9%; standard error ± 4.4%; $P = .038$; Figure 3A) but not reduced overall survival (supplemental Figure 7). Patients with *BRAF*^{V600E} mutations also more frequently received second-line systemic therapy (29.1% vs 15.8%; supplemental Table 7). When patients were stratified by disease extent, however, *BRAF*^{V600E} no longer associated with outcome parameters like EFS (Figure 3B-D). Children with *BRAF*^{V600E} mutations particularly had noninferior EFS in the subgroups of patients with SS-UFB disease (Figure 3D) or SS-MFB LCH (supplemental Figure 8), representing almost two-thirds of all patients (66%) in our cohort. In addition, disease extent but not lesional *BRAF*^{V600E} status was associated with EFS in multivariable survival analysis of the overall cohort (*BRAF*^{V600E}, hazard ratio, 1.08; 95% CI, 0.75-1.55; $P = .67$; supplemental Table 8).

MAP2K1 and *BRAF* exon 12 mutations in relation to clinical outcome

Follow-up was similar for patients with *BRAF*^{V600E}, *MAP2K1*, and *BRAF* exon 12 mutations (median, 4.0 years vs 3.7 years vs 5.3 years, respectively; $P = .87$). No significant differences in EFS were observed between the 3 molecular subgroups, particularly after patient stratification by disease extent (Figure 3E-F; supplemental Figure 8). Incidence of DI was similar among children with *BRAF*^{V600E} or *BRAF* exon 12 mutations (12.0% vs 12.8%) and higher than among children with *MAP2K1* mutations (3.7%), although not statistically significant (Tables 1 and 2; supplemental Table 6).

Clinical features of patients with LCH with alternative MAPK pathway gene alterations

Rare MAPK pathway gene alterations were identified in 16 patients without *BRAF*^{V600E} (supplemental Tables 2 and 11). Ten children had a *BRAF* exon 15 mutation other than *BRAF*^{V600E}, including 6 with a *BRAF*^{V600D} mutation,[52] and single cases with a *BRAF* p.T599_V600insEAT, *BRAF* p.T599_V600insEKST, *BRAF* p.V600_R603delinsEKSQ, or *BRAF* p.V600_W604delinsESRG mutation. All 6 patients with *BRAF*^{V600D} had SS-bone LCH (either UFB or MFB); none of them developed disease in another organ system during follow-up (median, 4.7 years; range, 0.6-12.6 years). However, several patients with *BRAF*^{V600D} mutations had uncommon abscess-like soft tissue extension through the skin (Figure 4E; supplemental Table 2).[53] The patient with the *BRAF* p.V600_R603delinsEKSQ mutation had MS-RO^{+} disease and required second- and third-line chemotherapy. *BRAF* fusions were identified in 3 patients using FFPE-TLC NGS (Figure 4A-D; supplemental Figure 10).[44] All 3 cases had different *BRAF* fusion partners, including *TMEM106B*, *DOCK8*, and *BICD2*. Two of 3 patients with *BRAF* rearrangements had SS-bone LCH without progression or relapse during their follow-up (5.4 or 27.5 years); the remaining patient with a *BICD2*::*BRAF* fusion had MS-RO^{-} disease with uncommon large tumors in both lungs (Figure 4G) instead of small nodules and cysts typical for pulmonary LCH.[54-56] This patient had progressive disease despite 2 lines of chemotherapy and recently received MEK inhibition (trametinib) with a complete metabolic response after 6 months of treatment. The *ARAF* and *KRAS* mutations were confined to patients with SS-bone LCH.

Additional MAPK pathway gene alterations were identified in 3 *BRAF*$^{V600E+}$ cases, including 1 previously reported patient with a *MAP3K1* mutation.[24] The other 2 cases had an additional *BRAF* p.R603Q mutation, previously also reported in another child with *BRAF*^{V600E}-mutated LCH.[17] One of our patients had SS-UFB LCH with multiple bone relapses during follow-up, requiring multiple lines of chemotherapy. The other patient had MS-RO^{+} disease and required second-line chemotherapy with cladribine because of progression of lung lesions. Eventually, all patients reached complete remission (supplemental Table 2).

Discussion

Through an international collaborative effort, we present here a large clinicogenomic study of childhood LCH. We confirm findings of previous research, most notably by Héritier et al,[10] but also reveal new associations of *BRAF* and *MAP2K1* mutations with clinical features at presentation (Table 3). In addition, we highlight that lesional *BRAF*^{V600E} status did not correlate with inferior clinical outcome after patient stratification by disease extent, a prognostic factor known for decades.[6-8]

Regarding *BRAF*^{V600E}, our study points at a potential association with a higher prevalence of gastrointestinal involvement (Table 1). Interestingly, gastrointestinal involvement was recently shown to provide additive unfavorable prognostic impact in patients with high-risk LCH.[61] Together, these data further support that *BRAF*^{V600E} associates with the most severe clinical presentations of pediatric LCH. *BRAF*^{V600E} also seemed more prevalent in patients with CNS-risk bone lesions; thus, *BRAF*^{V600E} now appears to associate with all disease characteristics known to correlate with clinical ND-LCH, including MS disease, skin and pituitary involvement, and CNS-risk bone lesions.[10,34,35,62] Accordingly, all 5 patients with clinical ND-LCH in our cohort harbored *BRAF*^{V600E} (Table 1) and had at least one of these disease characteristics. Although we confirm that *BRAF*^{V600E} correlates with reduced EFS in the overall cohort,[10] we show that this is (primarily) driven by the association of *BRAF*^{V600E} with disease extents known for high rates of progression or relapse (supplemental Figure 11), including MS LCH and SS-multifocal skin disease (supplemental Figure 9). This insight did not emerge from the study by Héritier et al[10] because the univariable survival analyses presented in their study were only stratified by RO involvement, with MS-RO^{-} and SS-multifocal skin disease still overrepresented in patients with *BRAF*^{V600E} in the low-risk disease subgroup (Figure 3B). Interestingly, lesional *BRAF*^{V600E} status also did not correlate with inferior clinical outcome in recent molecular studies of adult LCH.[31,63-65] Thus, the quest for independent prognostic factors in LCH continues.

Our study confirms that *MAP2K1* mutations in pediatric LCH predominantly occur in exon 2, affecting the αA-helix of MEK1 (Figure 5; supplemental Figure 12),[66,67] with p.Q58_E62del as the most detected mutation (supplemental Table 9).[19] The distinction between *MAP2K1* exon 2 or 3 mutations is important because the mutations in exon 2 are RAF-regulated, whereas the deletions in exon 3 are RAF and phosphorylation independent.[68] Consequently, these *MAP2K1* exon 3 deletions are less sensitive

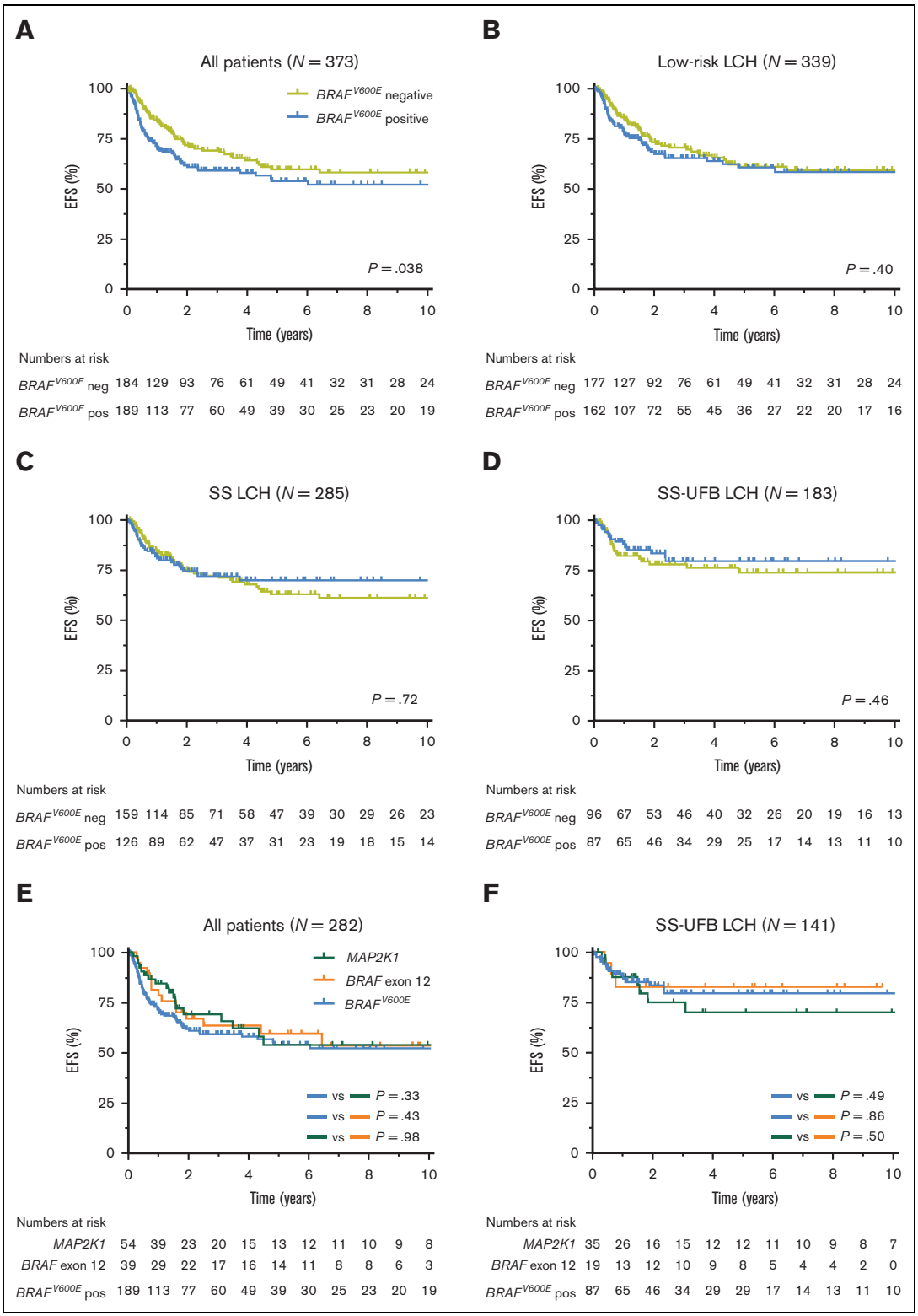

Figure 3. Clinical outcome of patients with pediatric LCH according to mutational status and disease extent. Kaplan-Meier curves showing EFS according to lesional *BRAF*^{V600E} status for all 373 patients (A), 339 patients with low-risk LCH (B), 285 patients with SS LCH (C), or 183 patients with SS-UFB LCH (D) at diagnosis. Patients with low-risk LCH comprise all patients except those with high-risk (MS-RO^{+}) disease. Kaplan-Meier curves showing EFS of patients with *BRAF*^{V600E}, *BRAF* exon 12, or *MAP2K1* mutations (E-F). Curves are shown for all 282 patients (E) and for 141 patients with SS-UFB LCH (F) at diagnosis. Four patients without clinical follow-up were not included in these survival analyses. pos, positive; neg, negative.

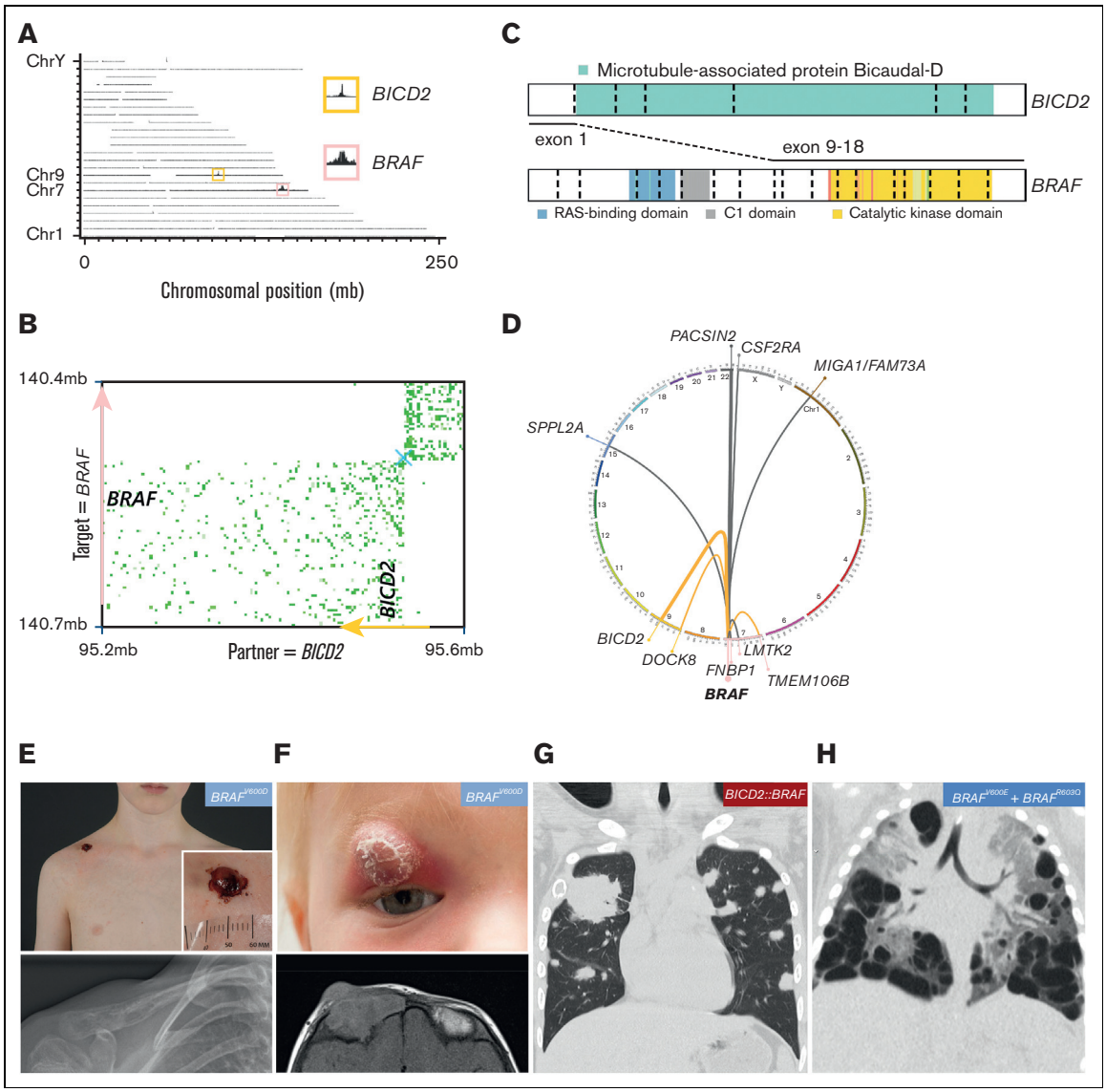

Figure 4. Molecular and clinical findings in patients with rare *BRAF* alterations. (A) Genome-wide coverage of fragments retrieved from a FFPE-TLC experiment targeting *BRAF* on a FFPE tissue sample from a patient from our cohort. A rearranged region to the *BRAF* gene (pink box) on chromosome 7 (Chr7) was identified by the concentration of fragments clustered around the *BICD2* gene (yellow box) on chromosome 9. (B) Butterfly plot uncovering the reciprocal *BICD2*::*BRAF* rearrangement. Proximity-ligation products between the target gene (*BRAF*) and rearrangement partner (*BICD2*) are depicted (in green). Strand directions are indicated by arrows. See supplemental Figure 10 for details about FFPE-TLC technology. (C) Illustration of the identified *BICD2*::*BRAF* fusion. (D) Circos plot depicting the 3 distinct *BRAF* rearrangements identified in patients from our cohort (in orange), as well as other *BRAF* rearrangements previously identified in patients with LCH (in gray).[17,25,57-59] (E) Clinical and conventional radiography images of a patient from our cohort with $BRAF^{V600D}$-mutated SS-UFB LCH, who had a single osteolytic lesion in the right clavicle with remarkable abscess-like soft tissue extension through the skin. (F) Clinical and magnetic resonance imaging images of a patient from our cohort with $BRAF^{V600D}$-mutated SS-MFB LCH, who had a relapse of MFB disease with a remarkable orbital lesion with clear skin changes. (G) Coronal image of a chest computed tomography scan showing atypical pulmonary lesions in the patient with a *BICD2*::*BRAF* fusion. Shown are multiple solid nodules in both lungs, including a very large tumor in the right upper lobe measuring 55 × 18 × 15 mm. A biopsy of this tumor excluded cooccurrence of lymphoma or another disease and revealed clusters of $CD1a^{+}$ $CD207^{+}$ cells, compatible with LCH. (H) Coronal image of a chest computed tomography scan showing many large cystic lung lesions in a child with high-risk LCH harboring both $BRAF^{V600E}$ and $BRAF^{R603Q}$ mutations. Professional illustration of panel C made by ProteinPaint software.[60] mb, megabase.

to allosteric MEK inhibitors, such as trametinib or cobimetinib.[67,68] In addition, these so-called "class 3 *MAP2K1* mutants" result in higher activation of downstream extracellular signal-regulated kinase (ERK) in vitro when compared with *MAP2K1* exon 2 mutations.[68] Therefore, one could hypothesize that *MAP2K1* exon 3 deletions might associate with a more severe clinical phenotype; however, only 1 out of 17 children in our cohort with these mutations had MS LCH (Table 2). In addition, their EFS was not significantly worse than of children with *MAP2K1* exon 2 mutations (supplemental Figure 13). In general, our study points out that *MAP2K1* mutations typically correlate with a less-severe clinical presentation of pediatric LCH, with

Table 3. Summary of key findings

Mutational status in relation to clinical presentation					
Significant associations ($P < 0.00125$)			**Potential associations ($P \geq 0.00125 - P < 0.05$)**		
BRAF^{V600E}	↑ Multisystem disease ↑ Multifocal SS-skin disease ↑ Risk organ involvement ↑ Skin involvement ↓ Age at diagnosis ↓ Upper extremity bone involvement	Confirming prior findings[10]	*BRAF*^{V600E}	↑ CNS-risk bone involvement ↑ Gastrointestinal involvement ↓ SS-MFB disease	New findings
			BRAF exon 12	↑ Lung involvement	
MAP2K1	↑ SS-bone disease	New findings			

Mutational status in relation to clinical outcome					
Significant associations ($P < 0.05$)			**No evidence for associations ($P \geq 0.05$)**		
BRAF^{V600E}	↓ EFS when analyzing the overall cohort ↑ 2nd line systemic therapy (overall cohort)	Confirming prior findings[10]	*BRAF*^{V600E}	Outcome in clinical subgroups, e.g. SS-UFB	Highlighted negative findings
			BRAF exon 12 *MAP2K1*	Outcome in overall cohort and subgroups	

For associations of *BRAF*^{V600E}, *BRAF*$^{V600E+}$ (n = 191) vs *BRAF*$^{V600E-}$ (n = 186) patients were compared. For associations of *MAP2K1* or *BRAF* exon 12 mutations, assignment is based on the statistical comparison of patients with *MAP2K1* mutations (n = 54) or *BRAF* exon 12 mutations (n = 39) with patients with *BRAF*^{V600E}, respectively. Associations of *MAP2K1* or *BRAF* exon 12 mutations required (1) a difference with patients with *BRAF*^{V600E} resulting in a Fisher exact test $P < .05$ (for potential associations) or $P < 0.00125$ (for significant associations) and (2) a difference between patients with *MAP2K1* and *BRAF* exon 12 mutations resulting in a Fisher exact test $P < .05$.

significantly more SS-bone LCH and less MS disease compared with *BRAF*^{V600E} (Figure 2).

BRAF exon 12 mutations predominantly comprised small in-frame deletions affecting the β3-αC loop of the BRAF protein (Figure 5; supplemental Figure 12).[25] Like in adult LCH,[63] *BRAF* p.N486_P490del was the most detected mutation (supplemental Table 10). In addition, insertions at the end of *BRAF* exon 12 affecting the αC-β4 loop (Figure 5) were detected in 12 patients.[48] These patients comprised 11 children with the *BRAF* p.R506_K507insLLR mutation, first described in 2 cases by Héritier et al,[28] and 1 child with a *BRAF* p.L505_R506insTLL mutation. Importantly, both β3-αC and αC-β4 loop mutations are resistant to first-generation BRAF inhibitors like vemurafenib.[25,28,46,48] In accordance with the 2 cases reported by Héritier et al,[28] the αC-β4 loop insertions predominantly occurred in children with SS-UFB LCH (Table 2). Yet, we also identified this mutation in 1 child with MS LCH that had multiple bone relapses and required 4 lines of chemotherapy, again demonstrating that (recurrent) mutations are not completely specific to 1 clinical form of the disease. Interestingly, *BRAF* exon 12 deletions affecting the β3-αC loop seemed to associate with a high prevalence of lung involvement. This is in accordance with molecular studies of adult LCH, which described the frequent presence of these mutations in patients with adult LCH with pulmonary involvement,[31,63,64] often in the context of MS disease. Thus, molecular analysis of *BRAF* exon 12 should be particularly applied in patients with pulmonary lesions,[54,56] which may inform LCH diagnosis and enable rational, targeted therapy.

Finally, alternative MAPK pathway gene alterations seemed related to some uncommon disease manifestations, since we observed rare abscess-like soft tissue extension in several patients with *BRAF*^{V600D} mutations and atypical solid lung lesions in our case with a *BICD2*::*BRAF* fusion. Notably, all 3 cases with a *BRAF* fusion had different fusion partners, which stands in contrast to the high prevalence of 1 specific *ALK* fusion partner (*KIF5B*) in patients with ALK^{+} histiocytosis.[69] Thus, comprehensive molecular techniques are essential for detection of these rare genetic variants; their identification may have clinical consequences, as illustrated by our *BICD2*::*BRAF*$^{+}$ case that received third-line systemic therapy with trametinib and obtained a complete metabolic response (supplemental Table 2).

Altogether, these data indicate that oncogenic mutation subtype appears an important, but not the sole, driver of heterogeneity in clinical presentation of pediatric LCH. With increasing access to targeted therapies, identification of the precise somatic driver alteration in patients that could benefit from these agents is important, as mutation subtype influences responsiveness to BRAF and MEK inhibitors. Factors other than mutation subtype seem more involved in driving heterogeneous outcomes within clinical subgroups. To this end, (longitudinal) assessment of mutant alleles in cellular or cell-free DNA derived from peripheral blood and/or bone marrow represents an interesting opportunity for prognostic staging and monitoring response to therapy.[70-79]

Why specific mutations associate with distinct LCH clinical presentations remains an interesting and important issue for further investigation.[80] Notably, specific genetic alterations also associate with distinct histiocytic entities,[17,69,81] again demonstrating the intimate relationship between molecular pathogenesis and clinical histiocytosis phenotype. Differential ERK activation inflicted by the different genetic alterations may play a role,[5,68] although this was not apparent for *MAP2K1* exon 2 vs exon 3 mutations in our cohort. In addition, the association of *BRAF*^{V600E} with severe clinical forms of LCH may rely on (thus far unknown) mediators or confounders, such as additional (epi)genomic alterations, tissue- or context-specific factors, and the mutated cell-of-origin (supplemental Figure 11). Although previous whole-exome sequencing studies have revealed infrequent additional genomic alterations in LCH,[17,22,25] several studies have indicated a distinct impact of *BRAF*^{V600E} on the LCH-lesional immune microenvironment.[37,82,83]

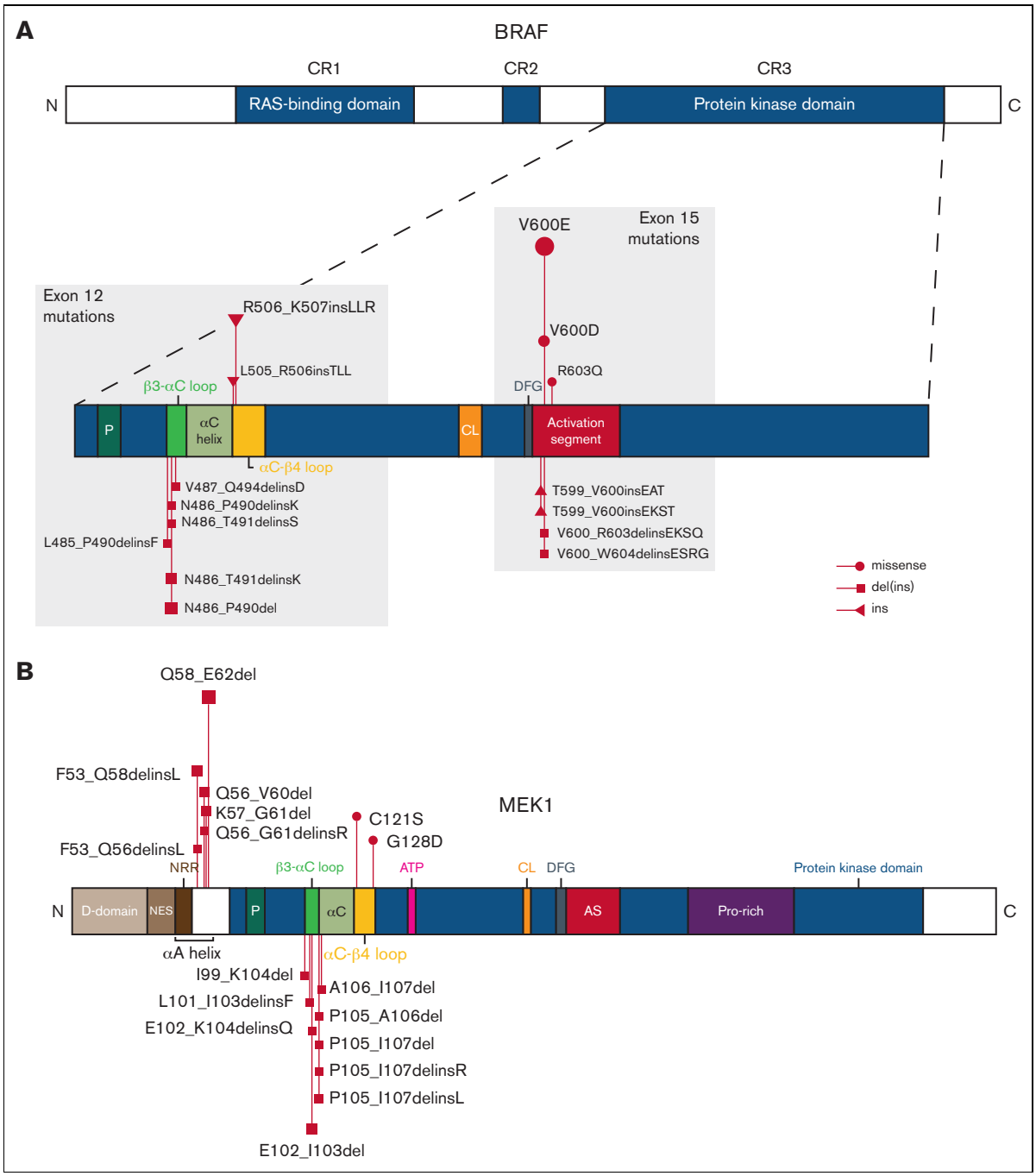

Figure 5. Identified BRAF and MEK1 alterations. Schematic representations of BRAF (A) and MEK1 (B) proteins with alterations detected in patients from our cohort. MEK1 is encoded by the gene *MAP2K1*. Figures not entirely to scale. AS, activation segment; ATP, adenosine triphosphate binding site; C, C-terminus; CL, catalytic loop; CR, conserved region; D, docking; del, deletion; DFG, DFG motif; ins, insertion; N, N-terminus; NES, nuclear export signal; NRR, negative regulatory region; P, phosphate-binding; Pro, proline.

Furthermore, several studies have suggested an important role for the mutated cell-of-origin in governing LCH clinical phenotype, with high-risk disease caused by mutations in multipotent hematopoietic stem/progenitor cells and low-risk disease caused by the same mutations in more committed myeloid precursors.[16,84,85] However, this simplified model also does not fully explain LCH clinical phenotype, as recent studies have identified mutation-carrying (myeloid and lymphoid) cells in the blood from patients with low-risk or even SS LCH.[41,84,86] Therefore, it remains important to elucidate how somatic mutations in multipotent progenitors can cause both SS and MS LCH and why progenitor cells active in children with high-risk LCH often harbor *BRAF*^{V600E}.

Limitations of our study include the fact that not all patients without *BRAF*^{V600E} were analyzed beyond *BRAF*^{V600E} (Figure 2A). Consequently, our study does not provide exact incidence rates of *MAP2K1*, *BRAF* exon 12, and rare MAPK pathway gene alterations. However, these alterations were detected in 109 children with LCH, allowing analysis of their clinical associations at unprecedented scale. Furthermore, because of the retrospective design, we cannot rule out some selection bias influencing the clinical spectrum of our cohort. However, our cohort included 288 (76.4%) patients with SS LCH compared with <70% in the study by Héritier et al,[10] strongly arguing against overrepresentation of patients with severe disease. Instead, we regard the relatively unbiased composition of our cohort as one of the strengths of our study. Nevertheless, our findings should be confirmed by sufficiently powered cohort studies; particularly the potential associations require further investigation (Table 3).

Overall, we present an international clinicogenomic study of childhood LCH, defining the clinical impact of recurrent *BRAF* and *MAP2K1* mutations. We demonstrate distinct associations of these driver mutation subtypes with demographic characteristics, disease extent, and specific sites of disease. Another key finding is that mutational status did not associate with EFS when patients were stratified by disease extent. These findings advance our understanding of factors underlying the remarkable clinical heterogeneity of pediatric LCH, and may guide molecular diagnostics beyond *BRAF*^{V600E}, for example, in children with (severe) lung involvement.[56]

Acknowledgments

The authors thank Elfriede Thiem, Femke Verwer, Merian van Overveld, Marije van der Waal, Esmée Berends, Marjon Wouters, Ingrid van der Geest, Karsten Nysom, Linda Warren, Veronica Lang, and Jill Beckley for their help with patient enrollment and/or clinical data collection. The authors also thank the Board of Histiocytose Nederland for their support. They thank Maria Luisa Coniglio, Konnie Hebeda, and Leonie Kroeze for providing molecular diagnostics data, Ronald van Eijk for providing TaqMan polymerase chain reaction reagents, Harma Feitsma for supervising formalin-fixed paraffin-embedded–targeted locus capture experiments performed at Cergentis BV, and professor Jelle Goeman for statistical advice.

This study was supported by grants from Histiocytosis Association of America (O.A., C.v.d.B., A.G.S.v.H.), Stichting 1000 Kaarsjes voor Juultje (A.G.S.v.H.), Stichting Kiwanis Run-for-LCH (A.G.S.v.H.), and Histio UK (T.v.W., A.G.S.v.H.).

P.G.K. received an MD/PhD grant from Leiden University Medical Center.

Supplemental Figures 1 and 5 and the visual abstract were made with BioRender.com software, and supplemental Figures 6 and 12 were made with the publicly available OncoPrinter and MutationMapper tools from cBioPortal for Cancer Genomics.[87,88]

Authorship

Contribution: A.G.S.v.H., C.v.d.B., J.A.M.v.L., O.A., and T.v.W. designed the study; C.v.d.B., O.A., J. Brok, T.v.B.G., K.S., A.B., J.A.M.v.L., C. Hutter, E. Sieni, and M.M. performed patient selection and enrollment; R.M.V., C.J.M.v.N., A.H.G.C., M.A.S.-V., M.J.K., L.K., and C. Hawkins provided tissue samples and/or routinely collected molecular diagnostic data; P.G.K., T.C.E.Z., C.v.d.B., O.A., I.T., R.M.E., J. Brok., T.v.B.G., K.S., A.B., J.A.M.v.L., C. Hutter, E. Sieni, M.M., and A.G.S.v.H. performed clinical data collection; H.B.A. performed LCH-IV clinical data extraction, and M.M. oversaw it; P.G.K., N.S.-W., J. Borst, E.C.S., D.v.E., J.F.S., E. Stelloo, C. Hutter, E. Sieni, T.v.W., and A.G.S.v.H. performed additional molecular genetic analyses; P.G.K. performed analysis of the combined clinicogenomic dataset and made the figures and tables; H.B.A. and U.P. supervised the statistical analyses; P.G.K. and A.G.S.v.H. drafted the manuscript; all authors as well as the DSMC of the LCH-IV clinical study approved the final version of the manuscript prior to submission.

Conflict-of-interest disclosure: J.F.S. and E. Stelloo are employees of Cergentis BV. The remaining authors declare no competing financial interests.

ORCID profiles: P.G.K., 0000-0001-9793-7032; T.C.E.Z., 0000-0003-2979-7044; N.S.-W., 0000-0002-3344-1799; J.F.S., 0000-0001-7030-6804; E. Stelloo, 0000-0002-1264-3594; I.T., 0000-0001-8106-8098; R.M.V., 0000-0003-1437-214X; C.J.M.v.N., 0000-0001-7907-7390; A.H.G.C., 0000-0002-3672-4348; M.A.S.-V., 0000-0001-8926-1140; L.K., 0000-0002-6113-6310; C. Hawkins, 0000-0003-2618-4402; R.M.E., 0000-0001-9852-0749; T.v.B.G., 0000-0001-6322-8035; K.S., 0000-0003-1267-4072; A.B., 0000-0002-6482-1823; J.A.M.v.L., 0000-0002-8885-4929; U.P., 0000-0001-7024-7082; C. Hutter, 0000-0003-2059-4814; E. Sieni, 0000-0002-6192-9812; M.M., 0000-0001-6471-8423; O.A., 0000-0001-7446-6274; T.v.W., 0000-0001-5773-7730; C.v.d.B., 0000-0002-6175-6077; A.G.S.v.H., 0000-0002-0563-4155.

Present address and correspondence: Astrid G. S. van Halteren, Department of Internal Medicine/Clinical Immunology, Erasmus MC, Dr. Molewaterplein 40, 3015 GD Rotterdam, The Netherlands; email: a.vanhalteren@erasmusmc.nl; and Cor van den Bos, Princess Máxima Center for Pediatric Oncology, 3720 AC Bilthoven, The Netherlands; email: c.vandenbos-5@prinsesmaximacentrum.nl.

References

1. Maarten Egeler R, van Halteren AGS, Hogendoorn PCW, Laman JD, Leenen PJM. Langerhans cell histiocytosis: fascinating dynamics of the dendritic cell-macrophage lineage. *Immunol Rev*. 2010;234(1):213-232.
2. Emile J-F, Abla O, Fraitag S, et al. Revised classification of histiocytoses and neoplasms of the macrophage-dendritic cell lineages. *Blood*. 2016;127(22):2672-2681.
3. Allen CE, Beverley PCL, Collin M, et al. The coming of age of Langerhans cell histiocytosis. *Nat Immunol*. 2020;21(1):1-7.

4. Allen CE, Merad M, McClain KL. Langerhans-cell histiocytosis. *N Engl J Med*. 2018;379(9):856-868.
5. Rodriguez-Galindo C, Allen CE. Langerhans cell histiocytosis. *Blood*. 2020;135(16):1319-1331.
6. Lahey ME. Prognostic factors in histiocytosis X. *Am J Pediatr Hematol Oncol*. 1981;3(1):57-60.
7. Ladisch S, Gadner H. Treatment of Langerhans cell histiocytosis–evolution and current approaches. *Br J Cancer Suppl*. 1994;23(70 (Suppl XXIII)):S41-S46.
8. Sterlich K, Minkov M. Childhood Langerhans Cell Histiocytosis: Epidemiology, Clinical Presentations, Prognostic Factors, and Therapeutic Approaches. *Rare Dis. - Diagnostic Ther. Odyssey*. 2021;4.
9. Haupt R, Minkov M, Astigarraga I, et al. Langerhans cell histiocytosis (LCH): guidelines for diagnosis, clinical work-up, and treatment for patients till the age of 18 years. *Pediatr Blood Cancer*. 2013;60(2):175-184.
10. Héritier S, Emile J-F, Barkaoui M-A, et al. BRAF mutation correlates with high-risk Langerhans cell histiocytosis and increased resistance to first-line therapy. *J Clin Oncol*. 2016;34(25):3023-3030.
11. Gadner H, Grois N, Pötschger U, et al. Improved outcome in multisystem Langerhans cell histiocytosis is associated with therapy intensification. *Blood*. 2008;111(5):2556-2562.
12. Gadner H, Minkov M, Grois N, et al. Therapy prolongation improves outcome in multisystem Langerhans cell histiocytosis. *Blood*. 2013;121(25):5006-5014.
13. Donadieu J, Bernard F, van Noesel M, et al. Cladribine and cytarabine in refractory multisystem Langerhans cell histiocytosis: results of an international phase 2 study. *Blood*. 2015;126(12):1415-1423.
14. Egeler RM, Katewa S, Leenen PJM, et al. Langerhans cell histiocytosis is a neoplasm and consequently its recurrence is a relapse: in memory of Bob Arceci. *Pediatr Blood Cancer*. 2016;63(10):1704-1712.
15. Badalian-Very G, Vergilio J-A, Degar BA, et al. Recurrent BRAF mutations in Langerhans cell histiocytosis. *Blood*. 2010;116(11):1919-1923.
16. Berres M-L, Lim KPH, Peters T, et al. BRAF-V600E expression in precursor versus differentiated dendritic cells defines clinically distinct LCH risk groups. *J Exp Med*. 2014;211(4):669-683.
17. Durham BH, Lopez Rodrigo E, Picarsic J, et al. Activating mutations in CSF1R and additional receptor tyrosine kinases in histiocytic neoplasms. *Nat Med*. 2019;25(12):1839-1842.
18. Hayase T, Saito S, Shioda Y, et al. Analysis of the BRAF and MAP2K1 mutations in patients with Langerhans cell histiocytosis in Japan. *Int J Hematol*. 2020;112(4):560-567.
19. Yang Y, Wang C, Wang D, et al. Clinical study of MAP2K1-mutated Langerhans cell histiocytosis in children. *J Cancer Res Clin Oncol*. 2022;148(9):2517-2527.
20. Feng S, Han L, Yue M, et al. Frequency detection of BRAF V600E mutation in a cohort of pediatric Langerhans cell histiocytosis patients by next-generation sequencing. *Orphanet J Rare Dis*. 2021;16(1):272.
21. Nelson DS, Quispel W, Badalian-Very G, et al. Somatic activating ARAF mutations in Langerhans cell histiocytosis. *Blood*. 2014;123(20):3152-3155.
22. Chakraborty R, Hampton OA, Shen X, et al. Mutually exclusive recurrent somatic mutations in MAP2K1 and BRAF support a central role for ERK activation in LCH pathogenesis. *Blood*. 2014;124(19):3007-3015.
23. Brown N, Furtado L, Betz B, Kiel M. High prevalence of somatic MAP2K1 mutations in BRAF V600E negative Langerhans cell histiocytosis. *Blood*. 2014;124(10):1655-1659.
24. Nelson DS, van Halteren A, Quispel WT, et al. MAP2K1 and MAP3K1 mutations in Langerhans cell histiocytosis. *Genes Chromosomes Cancer*. 2015;54(6):361-368.
25. Chakraborty R, Burke TM, Hampton OA, et al. Alternative genetic mechanisms of BRAF activation in Langerhans cell histiocytosis. *Blood*. 2016;128(21):2533-2537.
26. Diamond EL, Durham BH, Haroche J, et al. Diverse and targetable kinase alterations drive histiocytic neoplasms. *Cancer Discov*. 2016;6(2):154-165.
27. Lee LH, Gasilina A, Roychoudhury J, et al. Real-time genomic profiling of histiocytoses identifies early-kinase domain BRAF alterations while improving treatment outcomes. *JCI Insight*. 2017;2(3):e89473.
28. Héritier S, Hélias-Rodzewicz Z, Chakraborty R, et al. New somatic BRAF splicing mutation in Langerhans cell histiocytosis. *Mol Cancer*. 2017;16(1):115.
29. Héritier S, Emile J-F, Hélias-Rodzewicz Z, Donadieu J. Progress towards molecular-based management of childhood Langerhans cell histiocytosis. *Arch Pediatr*. 2019;26(5):301-307.
30. McGinnis LM, Nybakken G, Ma L, Arber DA. Frequency of MAP2K1, TP53, and U2AF1 mutations in BRAF-mutated Langerhans cell histiocytosis. *Am J Surg Pathol*. 2018;42(7):885-890.
31. Jouenne F, Chevret S, Bugnet E, et al. Genetic landscape of adult Langerhans cell histiocytosis with lung involvement. *Eur Respir J*. 2020;55(2):1901190.
32. Kemps PG, Hebeda KM, Pals ST, et al. Spectrum of histiocytic neoplasms associated with diverse haematological malignancies bearing the same oncogenic mutation. *J Pathol Clin Res*. 2021;7(1):10-26.
33. Ronceray L, Pötschger U, Janka G, Gadner H, Minkov M. Pulmonary involvement in pediatric-onset multisystem Langerhans cell histiocytosis: effect on course and outcome. *J Pediatr*. 2012;161(1):129-133.e3.

34. Grois N, Pötschger U, Prosch H, et al. Risk factors for diabetes insipidus in Langerhans cell histiocytosis. *Pediatr Blood Cancer*. 2006;46(2):228-233.
35. Grois N, Fahrner B, Arceci RJ, et al. Central nervous system disease in Langerhans cell histiocytosis. *J Pediatr*. 2010;156(6):873-881.e1.
36. Chellapandian D, Shaikh F, van den Bos C, et al. Management and outcome of patients with Langerhans cell histiocytosis and single-bone CNS-risk lesions: a multi-institutional retrospective study. *Pediatr Blood Cancer*. 2015;62(12):2162-2166.
37. Kemps PG, Zondag TC, Steenwijk EC, et al. Apparent lack of BRAFV600E derived HLA class I presented neoantigens hampers neoplastic cell targeting by CD8+ T cells in Langerhans cell histiocytosis. *Front Immunol*. 2020;10:3045.
38. Melloul S, Hélias-Rodzewicz Z, Cohen-Aubart F, et al. Highly sensitive methods are required to detect mutations in histiocytoses. *Haematologica*. 2019;104(3):e97-e99.
39. van Eijk R, Licht J, Schrumpf M, et al. Rapid KRAS, EGFR, BRAF and PIK3CA mutation analysis of fine needle aspirates from non-small-cell lung cancer using allele-specific qPCR. *PLoS One*. 2011;6(3):e17791.
40. van Eijk R, Stevens L, Morreau H, van Wezel T. Assessment of a fully automated high-throughput DNA extraction method from formalin-fixed, paraffin-embedded tissue for KRAS, and BRAF somatic mutation analysis. *Exp Mol Pathol*. 2013;94(1):121-125.
41. Xiao Y, van Halteren AGS, Lei X, et al. Bone marrow–derived myeloid progenitors as driver mutation carriers in high- and low-risk Langerhans cell histiocytosis. *Blood*. 2020;136(19):2188-2199.
42. Cohen D, Hondelink LM, Solleveld-Westerink N, et al. Optimizing mutation and fusion detection in NSCLC by sequential DNA and RNA sequencing. *J Thorac Oncol*. 2020;15(6):1000-1014.
43. de Vree PJP, de Wit E, Yilmaz M, et al. Targeted sequencing by proximity ligation for comprehensive variant detection and local haplotyping. *Nat Biotechnol*. 2014;32(10):1019-1025.
44. Allahyar A, Pieterse M, Swennenhuis J, et al. Robust detection of translocations in lymphoma FFPE samples using targeted locus capture-based sequencing. *Nat Commun*. 2021;12(1):3361.
45. Schemper M, Smith TL. A note on quantifying follow-up in studies of failure time. *Control Clin Trials*. 1996;17(4):343-346.
46. Chen S-H, Zhang Y, Van Horn RD, et al. Oncogenic BRAF deletions that function as homodimers and are sensitive to inhibition by RAF dimer inhibitor LY3009120. *Cancer Discov*. 2016;6(3):300-315.
47. Foster SA, Whalen DM, Özen A, et al. Activation mechanism of oncogenic deletion mutations in BRAF, EGFR, and HER2. *Cancer Cell*. 2016;29(4):477-493.
48. Yap J, Deepak RNVK, Tian Z, et al. The stability of R-spine defines RAF inhibitor resistance: a comprehensive analysis of oncogenic BRAF mutants with in-frame insertion of αC-β4 loop. *Sci Adv*. 2021;7(24):eabg0390.
49. Ducassou S, Seyrig F, Thomas C, et al. Thymus and mediastinal node involvement in childhood Langerhans cell histiocytosis: long-term follow-up from the French national cohort. *Pediatr Blood Cancer*. 2013;60(11):1759-1765.
50. Picarsic J, Egeler RM, Chikwava K, Patterson K, Jaffe R. Histologic patterns of thymic involvement in Langerhans cell proliferations: a clinicopathologic study and review of the literature. *Pediatr Dev Pathol*. 2015;18(2):127-138.
51. Yao J-F, Wang D, Ma H-H, et al. Characteristics and treatment outcomes of pediatric Langerhans cell histiocytosis with thymic involvement. *J Pediatr*. 2022;244(0):194-202.e5.
52. Kansal R, Quintanilla-Martinez L, Datta V, et al. Identification of the V600D mutation in Exon 15 of the BRAF oncogene in congenital, benign Langerhans cell histiocytosis. *Genes Chromosomes Cancer*. 2013;52(1):99-106.
53. Janssen LJF, Brons PPT, Schreuder HWB, et al. Image gallery: a rare abscess-like presentation of Langerhans cell histiocytosis. *Br J Dermatol*. 2017;176(4):e33.
54. Kambouchner M, Emile J-F, Copin M-C, et al. Childhood pulmonary Langerhans cell histiocytosis: a comprehensive clinical-histopathological and BRAFV600E mutation study from the French national cohort. *Hum Pathol*. 2019;89:51-61.
55. Della Valle V, Donadieu J, Sileo C, et al. Chest computed tomography findings for a cohort of children with pulmonary Langerhans cell histiocytosis. *Pediatr Blood Cancer*. 2020;67(10):e28496.
56. Le Louet S, Barkaoui M-A, Miron J, et al. Childhood Langerhans cell histiocytosis with severe lung involvement: a nationwide cohort study. *Orphanet J Rare Dis*. 2020;15(1):241.
57. Zarnegar S, Durham BH, Khattar P, et al. Novel activating BRAF fusion identifies a recurrent alternative mechanism for ERK activation in pediatric Langerhans cell histiocytosis. *Pediatr Blood Cancer*. 2018;65(1):e26699.
58. Zanwar S, Abeykoon JP, Dasari S, et al. Clinical and therapeutic implications of BRAF fusions in histiocytic disorders. *Blood Cancer J*. 2022;12(6):97.
59. Zhang R, Wang C-J, Zhao Y-Z, et al. Genetic landscape and its prognostic significance in children with Langerhans cell histiocytosis. *Pediatr Blood Cancer*. 2022;69(S1):S28-S29, e29453.
60. Zhou X, Edmonson MN, Wilkinson MR, et al. Exploring genomic alteration in pediatric cancer using ProteinPaint. *Nat Genet*. 2016;48(1):4-6.
61. Minkov M, Pötschger U, Thacker N, et al. Additive prognostic impact of gastrointestinal involvement in severe multisystem Langerhans cell histiocytosis. *J Pediatr*. 2021;237:65-70.e3.
62. Héritier S, Barkaoui M-A, Miron J, et al. Incidence and risk factors for clinical neurodegenerative Langerhans cell histiocytosis: a longitudinal cohort study. *Br J Haematol*. 2018;183(4):608-617.
63. Chen J, Zhao A-L, Duan M-H, et al. Diverse kinase alterations and myeloid-associated mutations in adult histiocytosis. *Leukemia*. 2022;36(2):573-576.

64. Cao X, Duan M, Zhao A, et al. Treatment outcomes and prognostic factors of patients with adult Langerhans cell histiocytosis. *Am J Hematol*. 2022;97(2):203-208.

65. Stathi D, Yavropoulou MP, Allen CE, et al. Prevalence of the BRAF V600E mutation in Greek adults with Langerhans cell histiocytosis. *Pediatr Hematol Oncol*. 2022;39(6):540-548.

66. Yuan J, Ng WH, Tian Z, et al. Activating mutations in MEK1 enhance homodimerization and promote tumorigenesis. *Sci Signal*. 2018;11(554):eaar6795.

67. Hanrahan AJ, Sylvester BE, Chang MT, et al. Leveraging systematic functional analysis to benchmark an in silico framework distinguishes driver from passenger MEK mutants in cancer. *Cancer Res*. 2020;80(19):4233-4243.

68. Gao Y, Chang MT, McKay D, et al. Allele-specific mechanisms of activation of MEK1 mutants determine their properties. *Cancer Discov*. 2018;8(5):648-661.

69. Kemps PG, Picarsic J, Durham BH, et al. ALK-positive histiocytosis: a new clinicopathologic spectrum highlighting neurologic involvement and responses to ALK inhibition. *Blood*. 2022;139(2):256-280.

70. Hyman DM, Diamond EL, Vibat CRT, et al. Prospective blinded study of BRAF V600E mutation detection in cell-free DNA of patients with systemic histiocytic disorders. *Cancer Discov*. 2015;5(1):64-71.

71. Héritier S, Hélias-Rodzewicz Z, Lapillonne H, et al. Circulating cell-free BRAF V600E as a biomarker in children with Langerhans cell histiocytosis. *Br J Haematol*. 2017;178(3):457-467.

72. Schwentner R, Kolenová A, Jug G, et al. Longitudinal assessment of peripheral blood BRAFV600E levels in patients with Langerhans cell histiocytosis. *Pediatr Res*. 2019;85(6):856-864.

73. Eckstein OS, Visser J, Rodriguez-Galindo C, Allen CE. Clinical responses and persistent BRAF V600E^{+} blood cells in children with LCH treated with MAPK pathway inhibition. *Blood*. 2019;133(15):1691-1694.

74. Donadieu J, Larabi IA, Tardieu M, et al. Vemurafenib for refractory multisystem Langerhans cell histiocytosis in children: an international observational study. *J Clin Oncol*. 2019;37(31):2857-2865.

75. Cui L, Zhang L, Ma H-H, et al. Circulating cell-free *BRAF* V600E during chemotherapy is associated with prognosis of children with Langerhans cell histiocytosis. *Haematologica*. 2020;105(9):e444-e447.

76. Wang C-J, Cui L, Ma H-H, et al. BRAF V600E Mutation in cell-free DNA, rather than in lesion tissues, at diagnosis is an independent prognostic factor in children with Langerhans cell histiocytosis. *Mol Cancer Therapeut*. 2021;20(7):1316-1323.

77. Poch R, Le Louet S, Hélias-Rodzewicz Z, et al. A circulating subset of BRAF ^{V600E} -positive cells in infants with high-risk Langerhans cell histiocytosis treated with BRAF inhibitors. *Br J Haematol*. 2021;194(4):745-749.

78. Eder SK, Schwentner R, Ben Soussia P, et al. Vemurafenib acts as a molecular on-off switch governing systemic inflammation in Langerhans cell histiocytosis. *Blood Adv*. 2022;6(3):970-975.

79. Kudo K, Toki T, Kanezaki R, et al. BRAF V600E-positive cells as molecular markers of bone marrow disease in pediatric Langerhans cell histiocytosis. *Haematologica*. 2022;107(7):1719-1725.

80. McClain KL, Chakraborty R. BRAF V600E vs cell of origin: what governs LCH? *Blood*. 2021;138(14):1203-1204.

81. McClain KL, Bigenwald C, Collin M, et al. Histiocytic disorders. *Nat Rev Dis Prim*. 2021;7(1):73.

82. Zeng K, Wang Z, Ohshima K, et al. BRAF V600E mutation correlates with suppressive tumor immune microenvironment and reduced disease-free survival in Langerhans cell histiocytosis. *OncoImmunology*. 2016;5(7):e1185582.

83. Sengal A, Velazquez J, Hahne M, et al. Overcoming T-cell exhaustion in LCH: PD-1 blockade and targeted MAPK inhibition are synergistic in a mouse model of LCH. *Blood*. 2021;137(13):1777-1791.

84. Milne P, Bigley V, Bacon CM, et al. Hematopoietic origin of Langerhans cell histiocytosis and Erdheim-Chester disease in adults. *Blood*. 2017;130(2):167-175.

85. Milne P, Abhyankar HA, Scull BP, et al. Cellular distribution of mutations and association with disease risk in Langerhans cell histiocytosis without BRAFV600E. *Blood Adv*. 2022;6(16):4901-4904.

86. Halbritter F, Farlik M, Schwentner R, et al. Epigenomics and single-cell sequencing define a developmental hierarchy in Langerhans cell histiocytosis. *Cancer Discov*. 2019;9(10):1406-1421.

87. Cerami E, Gao J, Dogrusoz U, et al. The cBio Cancer Genomics Portal: an open platform for exploring multidimensional cancer genomics data [figure]. *Cancer Discov*. 2012;2(5):401-404.

88. Gao J, Aksoy BA, Dogrusoz U, et al. Integrative analysis of complex cancer genomics and clinical profiles using the cBioPortal. *Sci Signal*. 2013;6(269):pl1.